# Elastic and Viscoelastic Properties of Cross-Linked Gold Nanoparticles Probed by AFM Bulge Tests

Hendrik Schlicke,[†] Elisabeth W. Leib,[†] Alexey Petrov,[†]

Jan H. Schröder,[†,‡] Tobias Vossmeyer*,[†]

## 1   Experimental setup

Figure S1 depicts the experimental setup used for pressure generation and control for bulging experiments. A gas cylinder was used to generate a nitrogen flow controlled by two needle valves, arranged in series. By adjusting the valves' orifices relatively, a pressure from 0 - 10 kPa could be set in between. The pressure was continuously recorded electronically by two digital pressure gauges for measurement ranges from 0 - 1 kPa and 0 - 10 kPa.
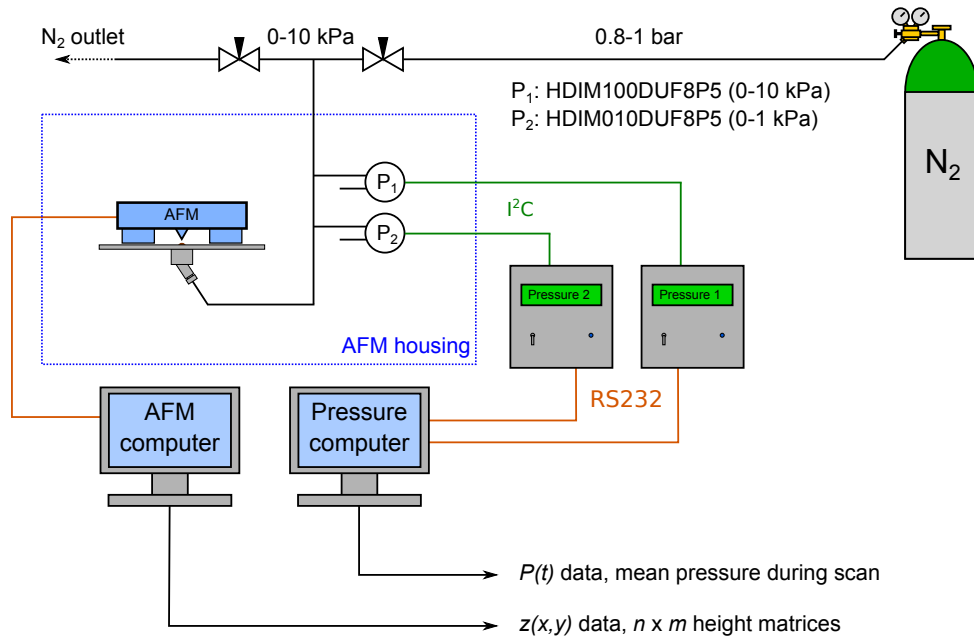


**Figure S1:** Schematic of the experimental setup used for pressure generation.

*To whom the correspondence should be addressed

[†]Institute of Physical Chemistry, University of Hamburg, Grindelallee 117, 20146 Hamburg, Germany. Email: tobias.vossmeyer@chemie.uni-hamburg.de

[‡]Present address: Physikalische Chemie I, Universität Bayreuth, Universitätsstr. 30, 95447 Bayreuth, Germany

# 2 Gold nanoparticles

A transmission electron micrograph and a size histogram of the gold nanoparticles used for film preparation are depicted in Figure S2. The range of particles' diameter included in the sizing statistics is $1\,\text{nm-}20\,\text{nm}$ ($0.78\,\text{nm}^2$-$314\,\text{nm}^2$). The particles showed an average diameter of $(3.8 \pm 0.6)$nm.
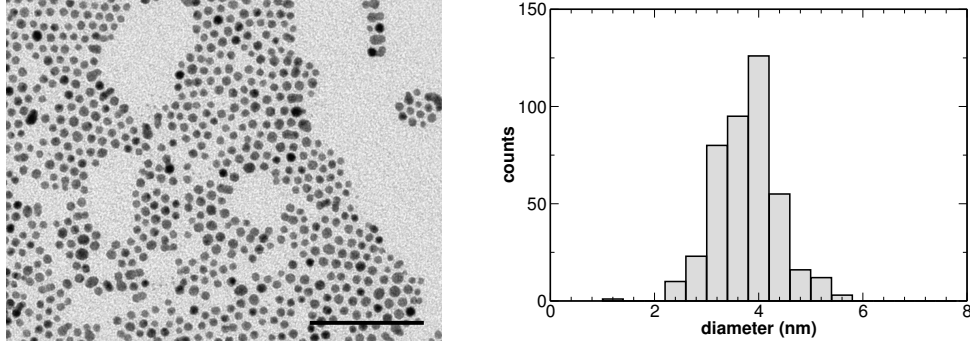


**Figure S2:** TEM micrograph (*scale bar:* 50 nm) *(left)* and size histogram obtained from TEM data *(right)*.

A UV/Vis spectrum of the gold nanoparticle sample is depicted in Figure S3. The solution was diluted by a factor of $f = 1/600$ for spectrum acquisition (optical path lengh: 1 cm). The spectrum shows the typical plasmon peak at a wavelength of $\lambda_{spr} = 514\,\text{nm}$.
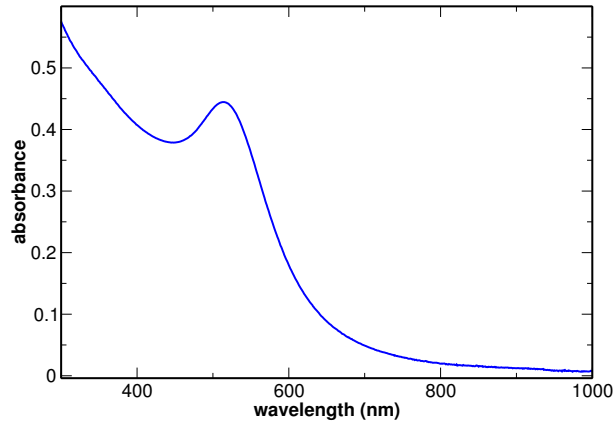


**Figure S3:** Absorbance spectrum of the diluted gold nanoparticle solution.

# 3   Substrate supported films

Figure S4 shows an exemplary AFM scan as used for thickness analysis of the membrane and an extracted height profile. Generally 10 profiles were extracted from two AFM scans at different positions to determine the membrane thickness.
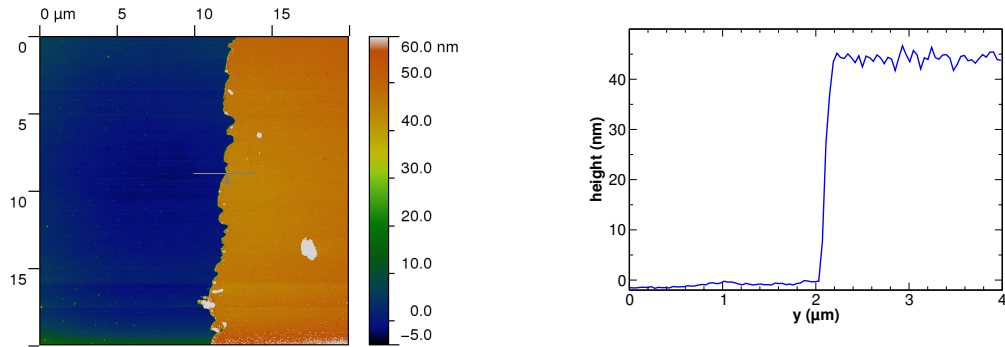


**Figure S4:** AFM scan of a substrate supported GNP film next to a scratch for determining the membrane thickness *(left)* and extracted step profile *(right)*.

Figure S5 shows UV/Vis spectra of substrate-supported GNP/NDT-films. The absorbance corresponds well with the thickness of the films.
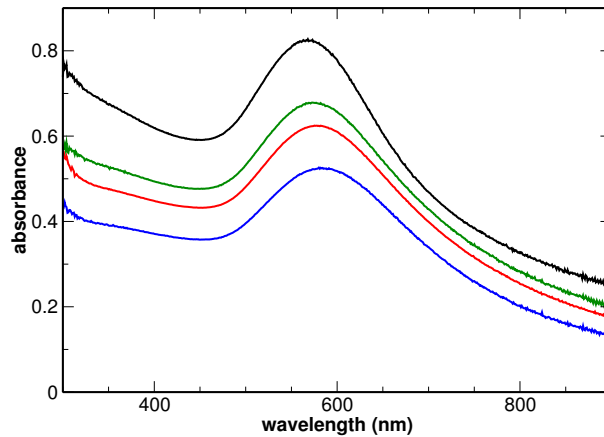


**Figure S5:** Plot of the substrate supported films' UV/Vis absorbance spectra. The membranes 31, 41, 44 and 60 are depicted as blue, red, green and black lines, respectively.

# 4 Data processing

Data processing was conducted using a custom python routine.

## 4.1 Peak-deflection method

For determining the correct central point deflection from the AFM profile scans (highlighted in Figure S6, right) it was necessary to correct for the tilt of the substrates. For this purpose a "full scan" of the membrane's dome was conducted for each sample, containing grid sections at all 4 edges. For taking into account the surface roughness, four areas (arranged in a square as highlighted in the exemplary topographic image S6, left) were used to calculate the slopes of the substrate in $x$- and $y$-direction. The average height values $\bar{z}_{11}$, $\bar{z}_{12}$, $\bar{z}_{21}$ and $\bar{z}_{22}$ for the respective areas were calculated.
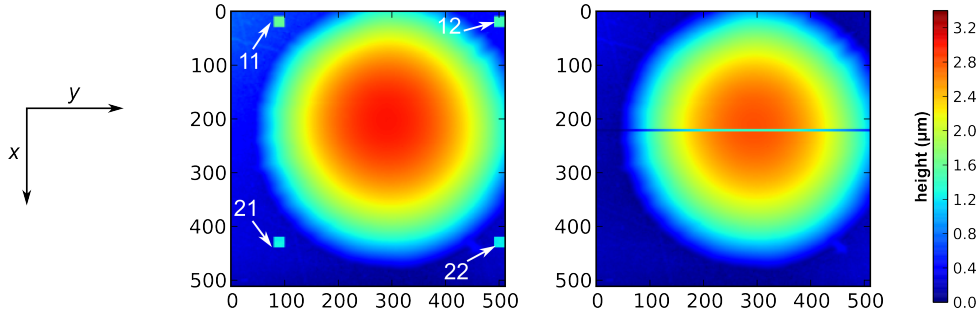


**Figure S6:** Exemplary depiction of the areas used for leveling the AFM scan data *(left)* and the 5-line profile scan *(right)*

Applying equations S1 and S2 the slopes of the substrate in $x$ and $y$ direction were obtained.

$$\bar{s}_x = \frac{\bar{z}_{21} - \bar{z}_{11} + \bar{z}_{22} - \bar{z}_{12}}{2(x_{21} - x_{11})} \tag{S1}$$

$$\bar{s}_y = \frac{\bar{z}_{12} - \bar{z}_{11} + \bar{z}_{22} - \bar{z}_{21}}{2(y_{12} - y_{11})} \tag{S2}$$

For (linear) tilt correction a tilt function S3 was subtracted from the topological AFM scan data obtained from the full AFM scan and the 5-line profile scans. The error due to this simplified tilt correction method is negligible for small tilts as found in these experiments.

$$Z_{tilt} = \bar{s}_x \ x + \bar{s}_y \ y \tag{S3}$$

The tilt-corrected 5-line profile scans recorded at different applied pressures ($Z_{profile}(x,y)$) (highlighted in the exemplary topographic AFM image in Figure S6, right) were then averaged to yield a profile $\bar{Z}_{profile}(y)$ along the fast scan ($y$-)direction (equation S4). This averaging was conducted to minimize the effect of surface roughness or noise on the measured deflections. Errors due to the width of the 5-line scan ($\Delta x = 0.977\,\mu$m) are negligible.

$$\bar{Z}_{profile}(y) = \frac{1}{5} \sum_{x=1}^{5} Z_{profile}(x,y) \tag{S4}$$

The height profiles' grid section was set to $z = 0$ by subtraction of $\bar{z}_{grid}$, the averaged height of the grid section next to the membranes' domes. Finally the central point deflection $h$ could be extracted by finding the maximum of the tilt- and offset-corrected profile:

$$h = \max\left(\bar{Z}_{profile}(y) - \bar{z}_{grid}\right) \tag{S5}$$

The obtained $h(P)$ data could be evaluated by fitting equation 1 described in the main text. Also, the obtained data could be converted into stress and strain ($\sigma(\varepsilon)$) acting on the membrane. From the central point deflection $h$ and the aperture radius $a$, the spherical cap's radius $R$ (see Figure 6 in the main document) could be computed following the geometrical equation S6.

$$R = \frac{a^2 + h^2}{2h} \tag{S6}$$

Using the equation for stress in a thin-walled spherical pressure vessel and equation S6 the biaxial stress in the membranes could be calculated for the respective $P(h)$ data points. Here, $t$ denotes the membrane thickness.

$$\sigma = \frac{PR}{2t} = \frac{P\left(a^2 + h^2\right)}{4ht} \tag{S7}$$

Also, the spherical cap's arc length could be computed applying the following equation:

$$s = \arctan\left(\frac{h}{a}\right)\frac{2\left(h^2 + a^2\right)}{h} \tag{S8}$$

Extrapolation of $\sigma(s)$ to $\sigma = 0$ yields $s_0$, the arc length at infinitesimal positive stress/pressure (of the unfolded membrane). The strain of the membrane can therefore be computed by:

$$\varepsilon = \frac{s}{s_0} - 1 \tag{S9}$$

The biaxial modulus obtained from the spherical cap model using the measured central point deflections can therefore be determined by fitting a slope function to the $\sigma(\varepsilon)$ data points:

$$\sigma = Y \cdot \varepsilon \tag{S10}$$

## 4.2 Circular-fit method

Evaluation of the bulge test data following the spherical cap model and the circular-fit method was conducted by fitting circles to the dome section of the line profiles as exemplarely shown in Figure S7. In this case tilt correction of the 5-line profile scans was not necessary.

The distance between a point of the scanned profile $\vec{r}_i$ to the center of the circle $\vec{r}_C$ to be fitted could be obtained as:

$$d_i = |\vec{r}_i - \vec{r}_C| \tag{S11}$$

The central coordinate of the optimized circle could be obtained by minimizing the deviation of the $d_i$-values following a least squares algorithm:

$$\min_{\vec{r}_C \to \vec{r}_{C,opt}} \sum_i \left( d_i - \frac{1}{N} \sum_j d_j \right)^2 \tag{S12}$$

The average distance between the optimized central point $\vec{r}_{C,opt}$ of the circle and the points of the line profile equals the radius $\bar{d}_{opt} = R$ of the idealized sphere.

From the radius $R$ and the applied pressure, the biaxial stress in the membrane could again be computed using the equation for stress in a thin-walled spherical pressure vessel S7.

Also the arc length $s$ could be computed using $R$ and the aperture radius $a$:

$$s = 2R \arcsin\left( \frac{a}{R} \right) \tag{S13}$$

Again $\sigma(s)$ was extrapolated to yield the spherical cap's arc length at infinitesimal positive stress $s_0$ and the strain was computed following equation S9. Finally, the biaxial modulus was again obtained by fitting a slope function (S10) to the $\sigma(\varepsilon)$ data points given by the circular-fit method.
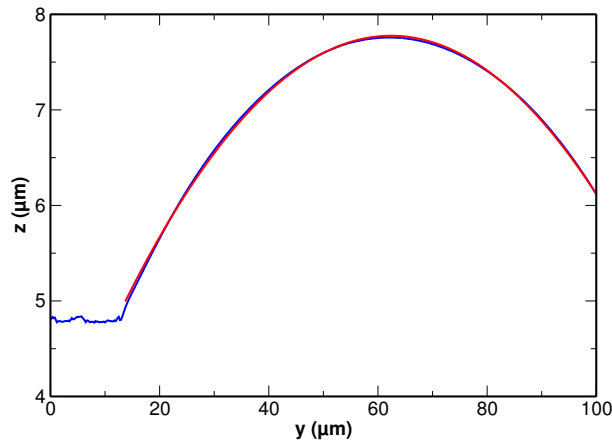


**Figure S7:** Line profile with fitted circle.

# 5 Additional data for analyzed samples
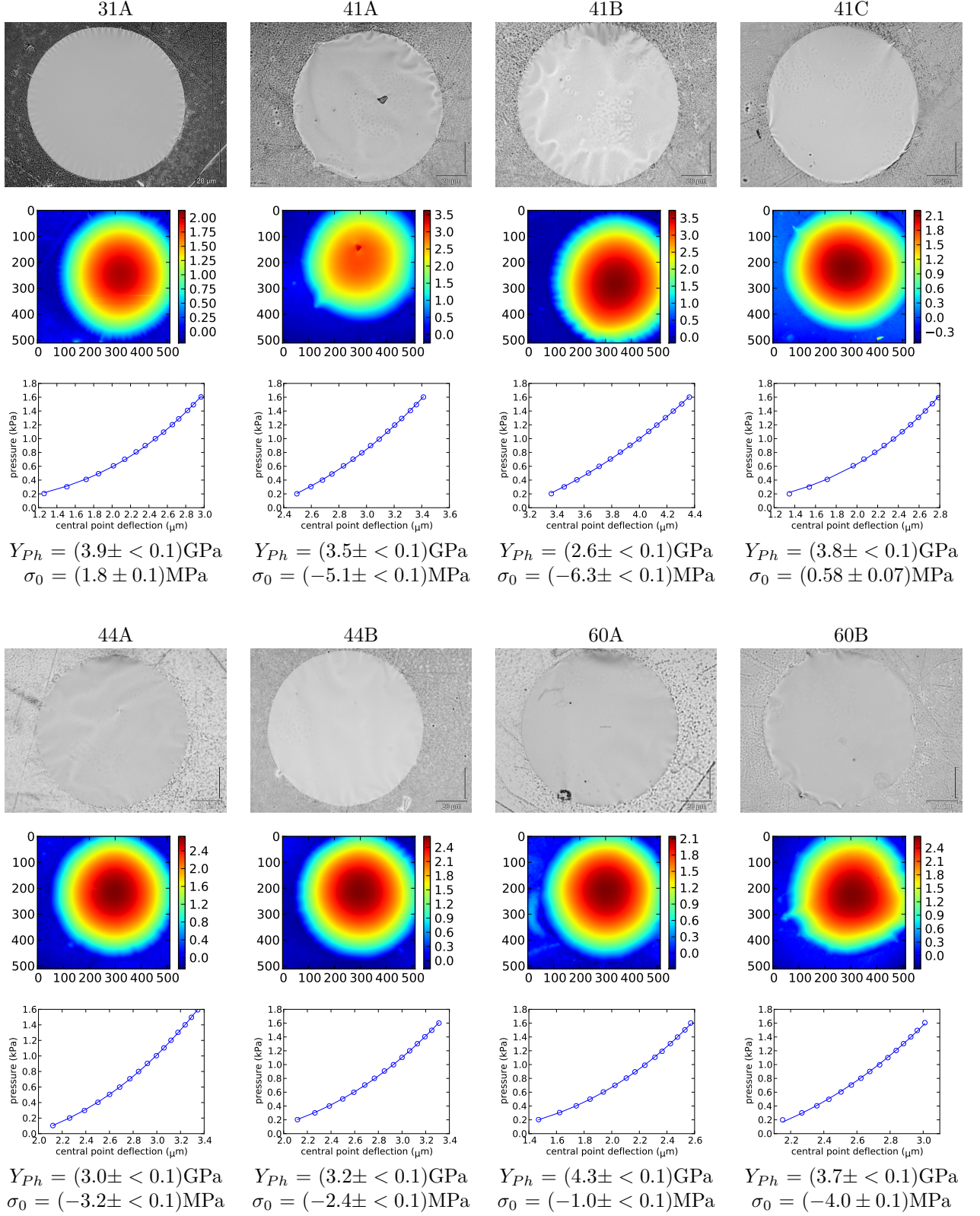


**Figure S8:** Optical micrographs *(top)* and leveled AFM full scans *(middle)* for bulge test samples analyzed in this study. AFM scans were acquired at an applied pressure of ∼0.7 kPa. Scale bars depicted in the optical micrographs are $20\,\mu$m. The area of the AFM full scans is $100 \times 100\,\mu\text{m}^2$ ($512 \times 512\,\text{px}^2$) and measured heights are given in $\mu$m (see plots' legends). The $P(h)$ data *(bottom)* were fitted with eq. 1 (see main document) yielding the biaxial modulus $Y_{Ph}$ and the residual sress $\sigma_0$.
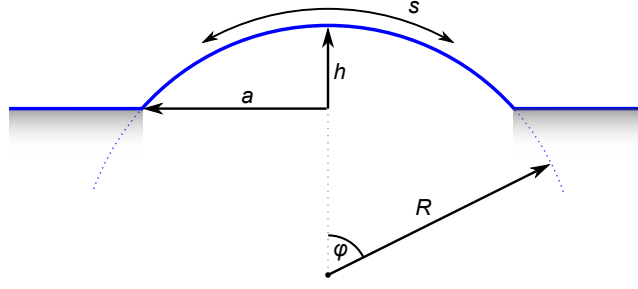
Stress-strain diagrams for the samples analyzed in this study are given in Figure S9.
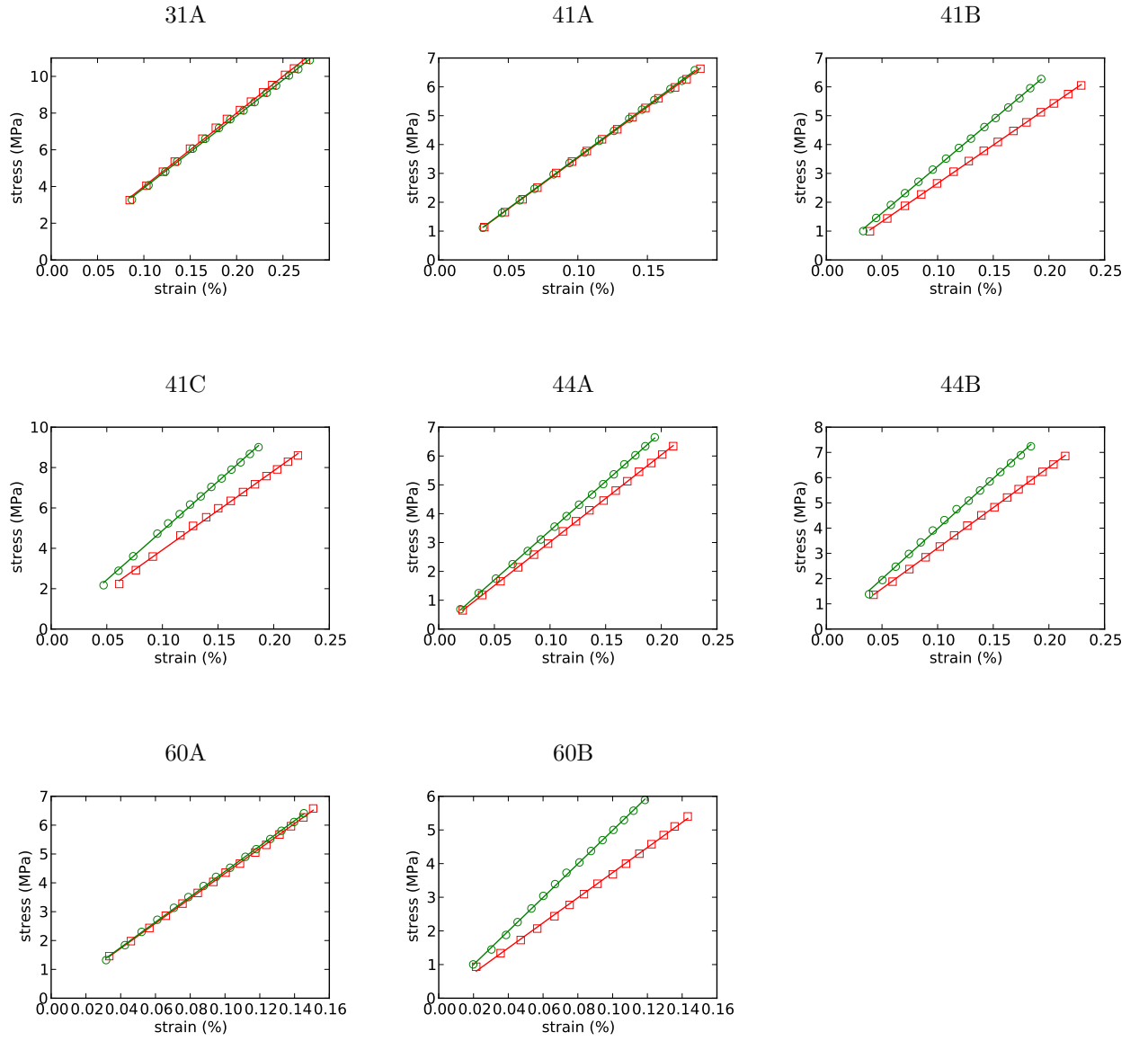


**Figure S9:** Stress-strain diagrams obtained for samples analyzed in this study. Red squares and green circles represent data points obtained by data processing according to the peak-deflection and circular-fit method, respectively. See Table 1 of the main document for the corresponding biaxial moduli.

**Table S1:** Comparative scheme of data processing methods, based on the spherical cap model, applied in this study. $t$ represents the membrane thickness, $P$ is the pressure, $\varepsilon$ the strain, $\sigma$ represents the biaxial stress and $Y$ is the biaxial modulus. Consider figure S10 for geometric definitions of the other parameters.

| method: | "circular-fit" | "peak-deflection" | "pressure vs. peak deflection plot" |
|---|---|---|---|
| input variables: | $R, P$ | $h, P$ | $h, P$ |
| calculation of $\sigma$: | $\sigma = \dfrac{PR}{2t}$ $(for\ t \ll R)$ | $\sigma = \dfrac{PR}{2t}$ $(for\ t \ll R)$ $\xrightarrow{\ R = \dfrac{a^2 + h^2}{2h}\ }$ $\sigma = \dfrac{P(a^2 + h^2)}{4th}$ | $\sigma = \dfrac{PR}{2t}$ $(for\ t \ll R)$ $\xrightarrow{\ R = \dfrac{a^2}{2h}\ (for\ h \ll a)\ }$ $\sigma = \dfrac{Pa^2}{4th}$ (eq. 1) |
| calculation of $\varepsilon$: | $\varepsilon = \dfrac{s}{s_0} - 1$ with: $s = 2\varphi R = 2R\arcsin\left(\dfrac{a}{R}\right)$ $s_0$ by extrapolation of $\sigma$ vs. $s$ to $\sigma(s_0) = 0$ | $\varepsilon = \dfrac{s}{s_0} - 1$ with: $s = 2\varphi R = \arctan\left(\dfrac{h}{a}\right)\dfrac{2(a^2 + h^2)}{h}$ $s_0$ by extrapolation of $\sigma$ vs. $s$ to $\sigma(s_0) = 0$ | $\varepsilon = \dfrac{s}{a} - 1 + \varepsilon_0 = \dfrac{R\varphi}{a} - 1 + \varepsilon_0$ ($\varepsilon_0$ : residual strain) $\xrightarrow{\ \varphi = \arcsin\left(\dfrac{a}{R}\right) \approx \dfrac{a}{R} + \dfrac{1}{6}\dfrac{a^3}{R^3}\ }$ (Taylor approximation) $\varepsilon = \dfrac{2h^2}{3a^2} + \varepsilon_0$ $\xrightarrow{\ \varepsilon_0 = \dfrac{\sigma_0}{Y}\ }$ ($\sigma_0$ : residual stress) $\varepsilon = \dfrac{2h^2}{3a^2} + \dfrac{\sigma_0}{Y}$ (eq. 2) |
| extraction of $Y$ and $\sigma_0$: | $\xrightarrow{}$ $\sigma = Y \cdot \varepsilon$ $Y$ is determined as slope of $\sigma(\varepsilon)$ plot | $\xrightarrow{}$ $\sigma = Y \cdot \varepsilon$ $Y$ is determined as slope of $\sigma(\varepsilon)$ plot | combining eq.s 1 and 2 with $\sigma = Y \cdot \varepsilon$ $P(h) = Y \cdot \dfrac{8t}{3a^4} \cdot h^3 + \sigma_0 \cdot \dfrac{4t}{a^2} \cdot h$ $Y$ and $\sigma_0$ are determined as fit-parameters of $P(h)$ plot |

9

**Figure S10:** Schematic depiction of the spherical cap model with annotated parameters used in Tab. S1.